ORNL/CP-98106

CONF-960643--

Roger E. Stoller[1]

THE IMPACT OF MOBILE POINT DEFECT CLUSTERS IN A KINETIC MODEL OF PRESSURE VESSEL EMBRITTLEMENT

REFERENCE: Stoller, R. E., "The Impact of Mobile Point Defect Clusters in a Kinetic Model of Pressure Vessel Embrittlement," Effects of Radiation on Materials: 18th International Symposium, ASTM 1325, R. K. Nanstad, M. L. Hamilton, F. A. Garner, and A. S. Kumar, Eds., American Society of Testing and Materials, 1997.

ABSTRACT: The results of recent molecular dynamics simulations of displacement cascades in iron indicate that small interstitial clusters may have a very low activation energy for migration, and that their migration is 1-dimensional, rather than 3-dimensional. The mobility of these clusters can have a significant impact on the predictions of radiation damage models, particularly at the relatively low temperatures typical of commercial, light water reactor pressure vessels (RPV) and other out-of-core components. A previously-developed kinetic model used to investigate RPV embrittlement has been modified to permit an evaluation of the mobile interstitial clusters. Sink strengths appropriate to both 1- and 3-dimensional motion of the clusters were evaluated. High cluster mobility leads to a reduction in the amount of predicted embrittlement due to interstitial clusters since they are lost to sinks rather than building up in the microstructure. The sensitivity of the predictions to displacement rate also increases. The magnitude of this effect is somewhat reduced if the migration is 1-dimensional since the corresponding sink strengths are lower than those for 3-dimensional diffusion. The cluster mobility can also affect the evolution of copper-rich precipitates in the model since the radiation-enhanced diffusion coefficient increases due to the lower interstitial cluster sink strength. The overall impact of the modifications to the model is discussed in terms of the major irradiation variables and material parameter uncertainties.

KEYWORDS: embrittlement, ferritic steels, hardening, modeling, molecular dynamics, point defects, pressure vessels, radiation damage, rate theory

---

The chemical reaction rate theory has been the primary tool used in modeling radiation-induced microstructural evolution for many years and the versatility of this theoretical framework is evident in its successful use in simulations of phenomena such as void swelling, irradiation creep, and embrittlement [1-10]. In order for radiation-induced

---

[1]Senior Research Staff Member, Metals and Ceramics Division, Oak Ridge National Laboratory, P. O. Box 2008, Oak Ridge, TN 37831-6376, USA

DISCLAIMER

microstructural evolution to occur, some mechanism must inhibit the complete recombination of the vacancies and interstitials being produced. In the conventional rate-theory models, the dislocation-interstitial bias provides the driving force for differential partitioning of the point defects. This bias arises because the elastic interaction between the strain fields of the dislocation and the interstitial leads to a higher dislocation capture efficiency for interstitials than for vacancies [11, 12]. A simple argument implies that if the dislocations absorb more interstitials than vacancies, the net climb can induce irradiation creep. Similarly, the supersaturation of vacancies remaining in the lattice can lead to vacancy clustering and these clusters may growth sufficiently large to induce void swelling.

Recently, an additional mechanism was proposed that could also contribute to point defect partitioning, the so-called production bias [13-15]. This mechanism depends on an asymmetry in the production of freely migrating interstitials and vacancies which arises from incascade point defect clustering and the different thermal stability of small vacancy and interstitial clusters. If a significant fraction of the interstitials produced by displacement cascades are found to cluster within the cascade and if these clusters are stable against interstitial emission, then a greater fraction of the vacancies than interstitials will escape the cascade in the form of mobile monodefects. This would lead to a vacancy supersaturation similar to that produced by the dislocation-interstitial bias.

The plausibility of this mechanism is supported by molecular dynamics (MD) displacement cascade simulations in which a high degree of incascade interstitial clustering has been observed. Cascade simulations have been carried out in a broad range of materials and the qualitative aspects of primary defect production are similar in each case [16-24]. A typical example of the MD results for iron is provided by ten 20 keV MD cascade simulations at 100 K. In this case, the average number of point defects that escaped intracascade annealing was 60 [21,22] or 30% of the number of defects that would be calculated using the standard NRT model [25]. Only about 40% of the interstitials were in the form of isolated monodefects; 60% were contained in clusters that had formed directly within the cascade. These incascade clusters contained from 2 to 13 interstitials. Information on the thermal stability of the clusters in iron was obtained in a detailed MD study of interstitial cluster stability by Wirth, et al. [26]. They reported that the binding energy of the last interstitial exceeded 1 eV for clusters containing from 2 to 25 interstitials.

However, the continuous production of stable interstitial clusters would quickly lead to an unrealistically high defect concentration and sink strength unless some mechanism existed for their removal from the system [10]. Indeed, this was one criticism of the production bias when it was initially proposed. The possibility of 1-dimensional (1D) loop motion as described by Trinkaus, et al. [15, 16] would permit the clusters to glide or diffuse to sinks. This proposal is consistent with the apparent interstitial cluster migration energies of less than a few tenths of an eV observed in MD simulations [20,26-28] and provides a plausible solution to this problem of interstitial cluster accumulation.

As discussed in References 20 and 23, the MD predictions appear to be in agreement with the limited experimental observations to which they can be directly compared. Although impurities and alloying elements are likely to alter some of the details observed, this general consistency of the MD results in different materials at least partially justifies the application of the MD results from pure metals in the embrittlement

model described below which was developed for the engineering alloys used in commercial reactor pressure vessels (RPV). This model was developed previously and has demonstrated reasonable agreement with Charpy data obtained from commercial fission reactor surveillance programs [7]. Here, the model will be used to examine the impact of interstitial cluster mobility on the embrittlement predictions. Detailed modeling requires the development of a self-consistent set of sink strengths to permit both 1D and 3D diffusion in the same model [15,16,29]. Because of uncertainties about the details of interstitial cluster migration, both 1D and 3D cluster motion will be examined separately.

EMBRITTLEMENT MODEL

The development and predictions of the basic embrittlement model is discussed in detail in Refs. 7 and 8; only a brief review will be presented here in order to provide a basis for discussing the changes required to implement interstitial cluster mobility. The impact of the revisions to the model will be shown by comparison with the previously published results.

This composite embrittlement model assumes that matrix hardening arises from two components: point defect clusters (PDC) and copper-rich precipitates (CRP). In the initial version, it is similar to models developed elsewhere [30-32]. A set of rate equations that describe the time or dose dependence of the interstitial and vacancy concentrations, the interstitial cluster population, the number of vacancy clusters, and the radius of the CRP is integrated. The hardening increment due to the PDC populations is computed assuming that they act as relatively weak dispersed barriers to dislocation motion, while the Russell-Brown model [33] is used to compute the hardening due to the CRP. Radiation-induced hardening values can be converted to equivalent shifts in the 41-J transition temperature (ΔT_{41}) through the use of correlation factors derived from irradiation experiments. For example, Odette and co-workers report yield strength to ΔT_{41} correlation factors ranging from 0.5 (plate) to 0.65 (weld) °C/MPa [30,34].

Using a set of reasonable physical parameters which are listed in part in Table 1 [7,8], the predictions of the model have shown reasonable agreement with ΔT_{41} data obtained from Charpy testing in commercial reactor surveillance programs. Figure 1 illustrates a typical comparison of the model and data on commercial welds form the Power Reactor Embrittlement Database [7,35]. In addition, the model has been used to examine the dependence of embrittlement on a broad range of material and irradiation parameters [7,8,36]. For example, the influence of the incascade clustering parameters is discussed in Ref. 36. The vacancy clustering fraction shown in Table 1 appears relatively high when compared to the minimal amount of incascade vacancy clustering which has been reported in MD cascade simulations in iron [19-22]. However, a recent reanalysis of the high-energy simulations indicates that the spatial arrangement of single vacancies is correlated out to at least the fourth nearest neighbor location when the simulations are terminated after 10 to 15 ps [27]. Since this time is too short to permit vacancy diffusion, the vacancy distribution can be thought of as containing a number of incipient vacancy clusters that could easily coalesce within the time required for a few vacancy jumps. Thus, the low reported vacancy clustering fractions could be a misleading result arising from the limited simulation time accessible by MD.

Table 1: Material parameters for ferritic steels

Parameter (units)	Symbol	Value
Cascade survival efficiency	η	0.1
Total interstitial clustering fraction	f_{icl}^T	0.3
Individual interstitial clustering fractions	f_2, f_3, f_4	0.15, 0.1, 0.05
Total vacancy clustering fraction	f_{vcl}	0.6
Incascade vacancy cluster radius (nm)	r_{vcl}	0.5
Interstitial migration energy (eV)	E_i^m	0.25
Vacancy migration energy (eV)	E_v^m	1.25
Vacancy formation energy (eV)	E_v^f	1.55
Network dislocation density (m^{-2})	ρ_n	0.5 to 5.0 x10^{14}
Dislocation capture efficiency: interstitials	Z_i^n	1.25
vacancies	Z_v^n	1.00
Dislocation barrier strength of PDC	α_B	0.25
Effective grain size (μm)	d_g	10.0

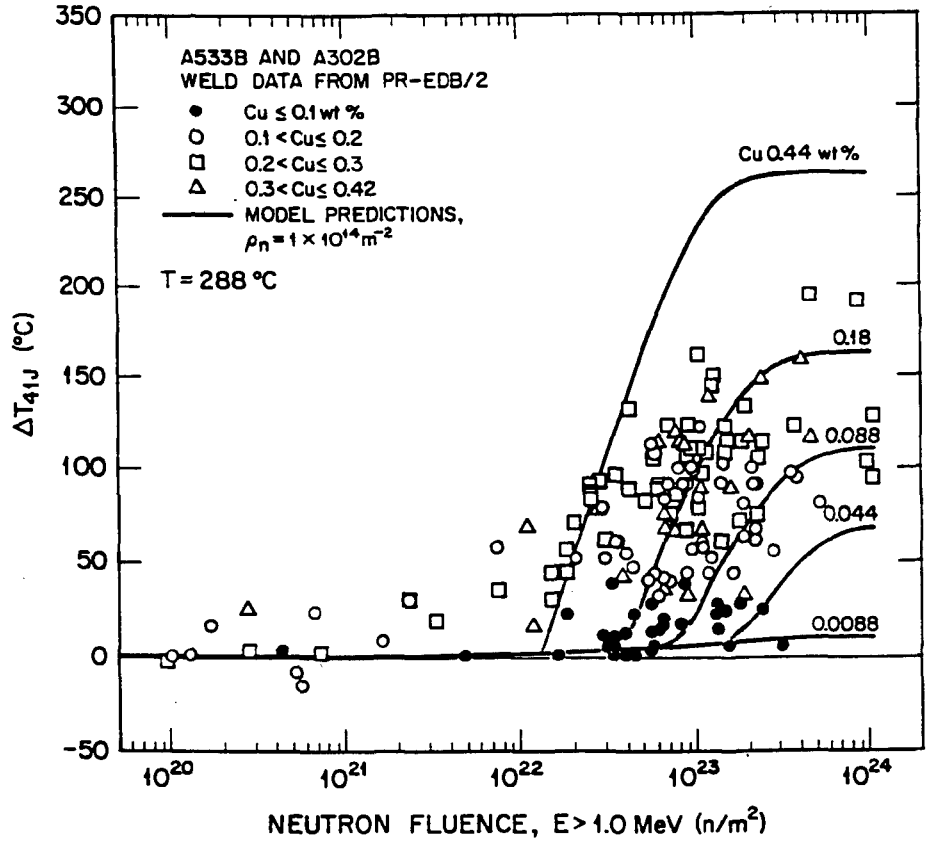

FIG. 1. Comparison of embrittlement model predictions and Charpy data from commercial reactor surveillance programs [7,35].

Interstitial Cluster Mobility: 3D

The modification of the model to include interstitial cluster mobility is reasonably straightforward if the clusters exhibit 3D diffusion. In this case, the sink strengths of the extended defects for the mobile clusters can be treated in the same way as for interstitials or vacancies. For simplicity, only the di- (C_2), tri- (C_3), and tetra (C_4) interstitial cluster sizes have been treated as mobile in this initial work. Much larger clusters have been observed to be mobile in the MD cascade simulations [20,21], and other MD work indicates that clusters containing up to 37 interstitials may migrate with an energy less than 0.25 eV [28]. The possibility of these clusters converting between glissile and sessile configurations is also not treated in this work. Thus, simulating the mobility of only the smallest interstitial clusters should be viewed as an initial attempt to investigate the sensitivity of the previous model to cluster mobility. Because of their mobility, the rate equations for C_2, C_3, and C_4 must be modified to reflect their absorption at sinks and their loss and creation by reactions between mobile clusters. Similarly, the equations for interstitial (C_i) and vacancy (C_v) concentrations must now include loss terms that account for the mobility of these small clusters.

The revised rate equations are illustrated below for C_i and C_2. Note that although the C_i notation has been retained from previous work, C_i=C_1 in the summations in these equations. Equations which include terms for the analogous reactions between the mobile defects and fixed sinks can be written for C_v, C_3, and C_4. The rate equations for the larger interstitial clusters are the same as described in Refs. 7 and 8, with the exception of additional terms for which account for the mobility of C_2, C_3, and C_4. The equation describing the lifetime of vacancy clusters was similarly modified to reflect the absorption rate of the mobile, multiple interstitial clusters.

$$\frac{dC_i}{dt} = G_i - \alpha C_i C_v - D_i C_i S_i^T - \sum_{j=1}^{j_{max}} \beta_i^j C_i C_j - \sum_{j=2}^{4} \beta_j^i C_j C_i, \qquad (1)$$

where the interstitial generation rate, G_i, is determined by the NRT atomic displacement rate, G_{dpa}; the cascade survival efficiency, η; and the total interstitial emission rate from di-, tri-, and tetra-interstitials, G_i^{em}. The total incascade interstitial clustering fraction, f_{icl}^T, is the sum of the di-, tri, and tetra-interstitial clustering fractions: f_2, f_3, and f_4,

$$G_i = \eta G_{dpa}(1 - f_{icl}^T) + G_i^{em}, \qquad (2)$$

$$G_i^{em} = E_2^i C_2 + E_3^i C_3 + E_4^i C_4 \qquad (3)$$

$$\frac{dC_2}{dt} = G_2 + \frac{\beta_i^i C_i}{2} + \beta_3^v C_v + \beta_v^3 C_3 \quad \ldots$$

$$- E_2^i C_2 - \beta_2^v C_v - \beta_v^2 C_2 - D_2 C_2 S_2^T - \sum_{j=1}^{j_{max}} \beta_2^j C_j - \sum_{j=1(\neq 2)}^{4} \beta_j^2 C_2 \qquad (4)$$

$$G_2 = \eta G_{dpa} f_2 + E_3^i C_3 \quad (5)$$

In both Eqns. (1) and (4), the first summation term accounts for reactions between the respective mobile defect and all other interstitial clusters, and the second summation accounts for the reactions between the other mobile clusters and the respective defect. This second sum begins at j=2 in Eqn. (1) and stipulates that j≠2 in Eqn. (4) to prevent double counting. The maximum interstitial cluster size (j_{max}) for the discrete cluster description is typically taken as 500 corresponding to a loop radius of ~3 nm. This accounts for the largest interstitial defects observed under the irradiation conditions of interest to RPVs. The additional terms requiring definition in Eqns. 1 to 5 are: α, the recombination coefficient; D_i and D_v, the interstitial and vacancy diffusivities; S_i^T and S_2^T, the total fixed sink strength for C_i and C_2; β_j^k, the rate at which mobile defect j encounters defect k; and E_j^i, the rate at which an interstitial is emitted from a cluster of size j. Unless otherwise described below, these terms are computed in the same way as in Refs. 7 and 8.

The fixed sinks represented by S_i^T and S_2^T include the dislocation network, the grain structure, and the vacancy clusters. In the examples that will be presented here, the sink strength for 3D diffusing interstitial clusters was taken to be the same as for mono-interstitials. The interstitial cluster migration energies will be used as a parameter for investigating the sensitivity of the model.

Interstitial Cluster Mobility: 1D

A detailed discussion of the issues involved in modeling 1D glide or diffusion is beyond the scope of this paper. A general treatment of the reaction rate parameters can be found in Ref. 29 and an initial application of the theory can be found in Refs. 15 and 16. However, an important difference between 3D and 1D diffusion can be understood by a simple geometric argument. The reaction cross section between a fixed sink and a defect moving in 1D is reduced because the defect is sampling a smaller volume of the material and revisits the same lattice sites more frequently than in a 3D random walk [37]. As a result, the mean range of a 1D gliding loop is increased or the effective sink strengths for capturing the loop are reduced relative to 3D diffusion. This effect increases for lower sink densities and the sink strength dependence is greater for dislocations than for cavities.

Since the concentrations of 1D migrating defects depend on the local, rather than the average sink concentration [38], the traditional effective medium approach strictly can not be applied to a system containing such defects. Recently, Singh and co-workers have presented a swelling model that includes both sessile and 1D glissile clusters, and details such as sessile-to-glissile cluster transformation [39]. Extension of their model may provide an improved approach; but, here the basic method used by Trinkaus, et al. [15, 16] was followed in modifying the embrittlement model for 1D diffusion.

The dislocation sink strength provides one example of the modified sink strengths. To lowest order, the 3D sink strength of a dislocation network is simply the dislocation density, $S_{3D}=\rho_n$ [m^{-2}]. If dislocations were the only sink, the mean range of a 3D migrating defect is given by the reciprocal square root of the sink strength, $\lambda_{3D}=(\rho_n)^{-0.5}$. The mean range for a 1D migrating defect is given as the product of the effective interaction diameter of the dislocation and the projection of the dislocation density in a

plane perpendicular to the 1D migration, $\lambda_{1D}=d_i \cdot \pi\rho_n/4$. The mean range in the presence of multiple sinks is calculated as the reciprocal sum of the range for individual sinks, and the 1D sink strength is similarly equal to $(\lambda_{1D})^{-2}$. The interaction diameter, d_i, can be obtained by an elasticity calculation [15, 16], and increases linearly with the number of point defects in the gliding cluster. Taking representative material parameters for a tetra-interstitial in a ferritic steel, the ratio of the mean range for 1D migration to 3D migration is about 14 for a dislocation density of 10^{15} m^{-2} and increases to 430 for a dislocation density of 10^{12} m^{-2}. The impact of this reduced sink strength will be shown below.

RESULTS AND COMPARISONS WITH PREVIOUS MODEL

Before describing the results of the modified model and making comparisons with the previous version, it is important to point out that quantitative comparisons are limited because the same material parameters were used in both cases. This permits the impact of cluster mobility to be assessed, but puts the modified model at a disadvantage when comparisons to experimental data are made. No attempt has yet been made to see if equivalent agreement between the predictions of the modified model and the data can be obtained through reasonable adjustment of other material parameters.

In order to illustrate the effects of both incascade clustering alone and cluster mobility, Figure 2 plots the calculated vacancy concentration at 0.01 dpa as a function of irradiation temperature for three cases: no incascade clustering, incascade clustering with immobile clusters, and incascade clustering with mobile clusters. In this third case the clusters are assumed to exhibit 3D migration with a migration energy of 0.25 eV. The most dramatic effect is that the sink strength arising from incascade clustering dramatically reduces the vacancy concentration at the temperatures below ~300°C. As discussed elsewhere [10], the very high vacancy concentrations obtained at the lower temperatures for the case without incascade clustering are probably nonphysical, and the existence of incascade clustering extends the useful range of the rate theory models. Weidersich has also discussed the importance of this cluster sink strength [40]. If the interstitial clusters exhibit 3D migration with a low activation energy, the cluster sink strength is reduced and the vacancy concentration rises accordingly.

The vacancy and interstitial cluster sink strength for these same three cases is shown in Figure 3, where the substantial changes in the total interstitial cluster sink strength (S_{icl}) are clearly visible. Absorption of mobile interstitial clusters gives rise to only a modest reduction in the vacancy cluster sink strength (S_{vcl}). The full range of calculated values are shown simply to demonstrate the sensitivity of the model. Clearly, sink strengths less than about 10^{10} m^{-2} are not physically significant, and the high cluster sink strengths calculated for the lowest temperatures may not be physically reasonable.

As a measure of their impact on mechanical properties, Figure 4 illustrates the effect of the interstitial cluster migration energy on the calculated hardening due to interstitial clusters. The increase in the shear strength on the dislocation glide plane is plotted as a function of dose, where the shear strength change is calculated as:

$$\Delta\tau = \alpha_B G b \left(\sum_j N_{icl} d_{icl}\right)^{0.5}, \qquad (6)$$

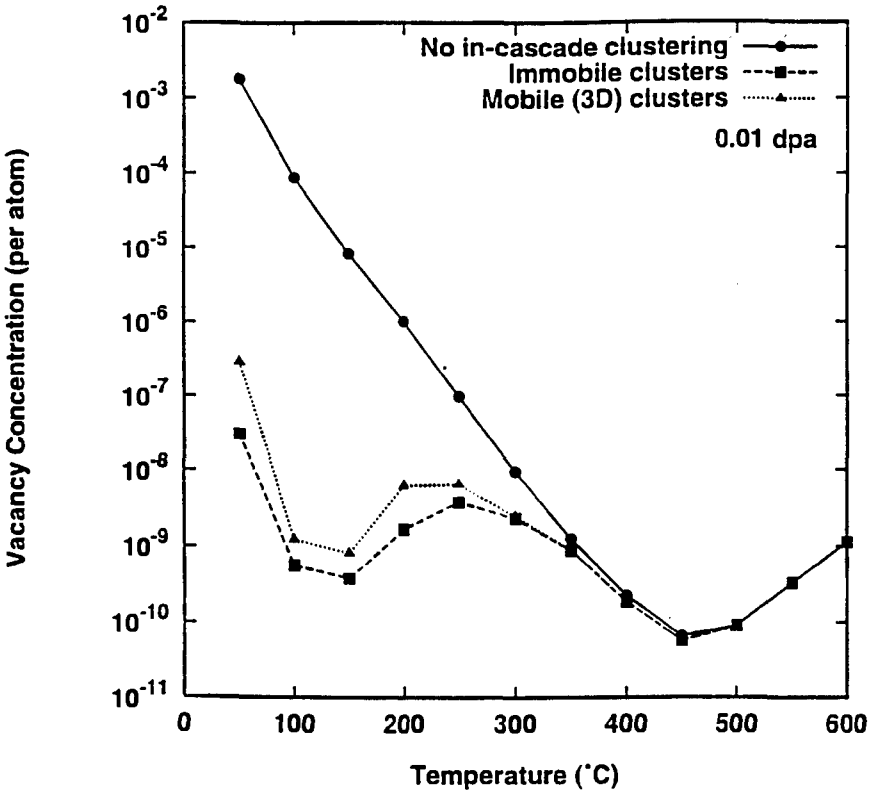

FIG 2. Influence of different assumptions regarding incascade clustering on the temperature dependence of the calculated vacancy concentration.

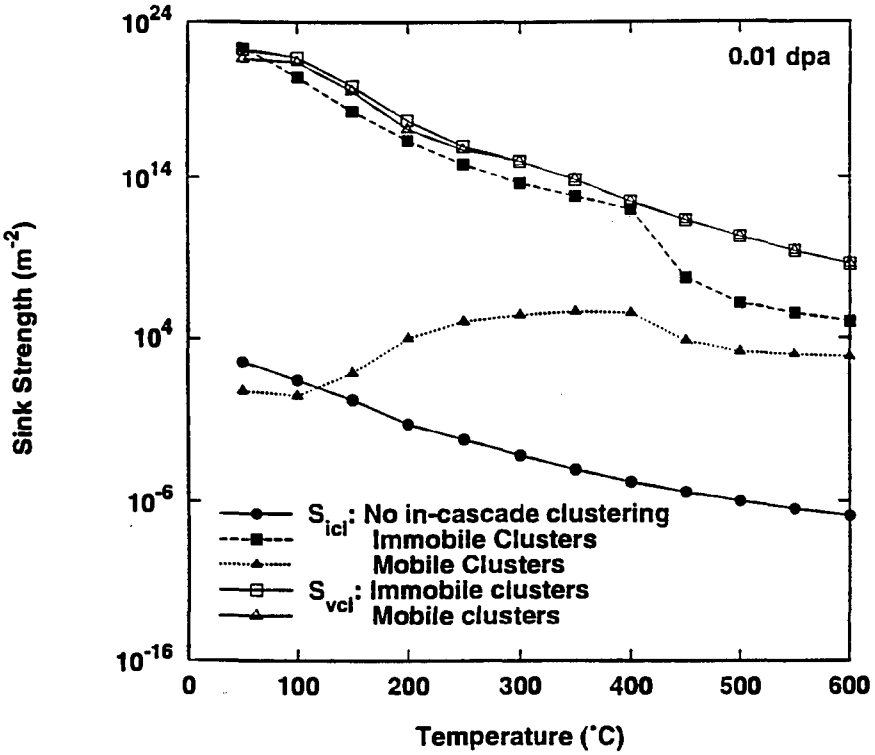

FIG 3. Influence of different assumptions regarding incascade clustering on the temperature dependence of the calculated interstitial and vacancy cluster sink strengths.

where α_B is the interstitial cluster barrier strength from Table 1, b is the magnitude of the Burger's vector, G is the shear modulus, and N_{icl} and d_{icl} are interstitial cluster number density and diameter in each size class, respectively. The subscript j in Eqn. (6) indicates summation only over the immobile interstitial cluster size classes. The solid curve labeled 'Base case' in Figure 4 is the prediction for case on immobile C_2, C_3, and C_4; whereas the migration energy indicated on the other curves was applied to all three mobile cluster sizes. The decrease in shear strength is consistent with the reduced sink strength shown in Figure 3, and it should be obvious that the very small strength increments are also not physically significant.

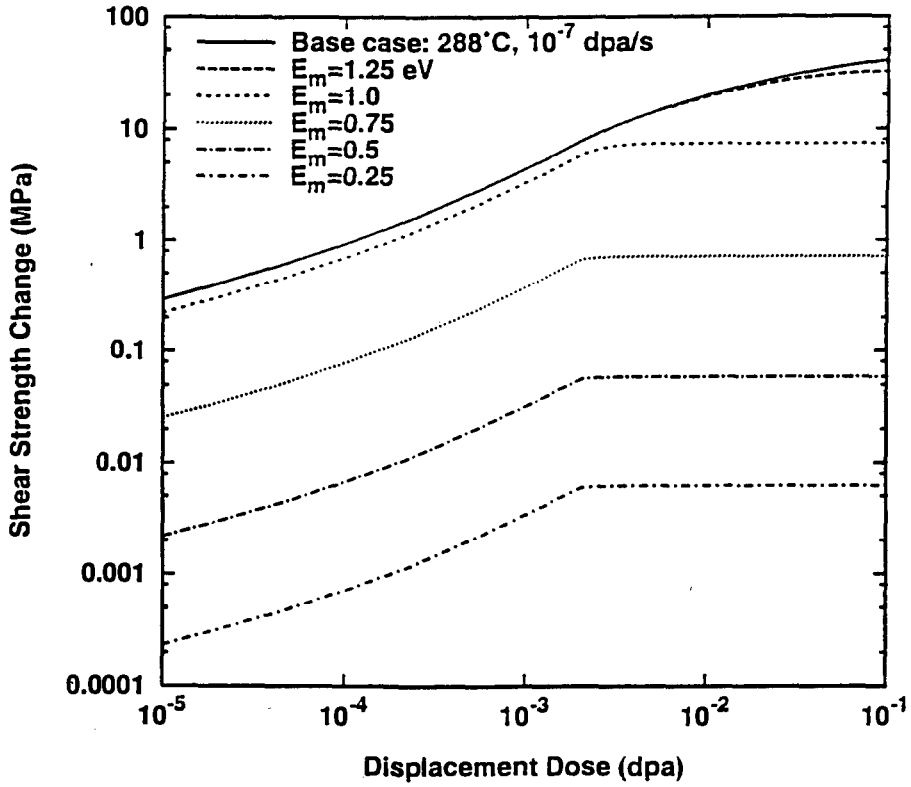

FIG. 4. Dose dependence of hardening due to interstitial clusters with various interstitial cluster migration energies.

Figure 5 provides a comparison of 1D and 3D interstitial cluster migration by showing the predicted yield strength change at 60°C as a function of dose for two displacement rates when either migration mechanism is invoked. This temperature is representative of commercial reactor support structures and the pressure vessel of some test reactors such as the High Flux Isotope Reactor (HFIR). As in Ref. 7, the shear strength change has been converted to a yield strength change by multiplying by the Taylor factor of 3.06. Once again, the "Base case" curve is that for immobile clusters. The lower displacement rate is that obtained in the surveillance program for the pressure vessel of the HFIR, and the higher rate is that of experiments that were conducted in the Oak Ridge Research Reactor (ORR) in an evaluation of the HFIR surveillance program. Data from HFIR surveillance program [41], the ORR irradiations [41], and additional irradiations conducted in the HFIR hydraulic tube are shown [42]. The displacement rate in these latter

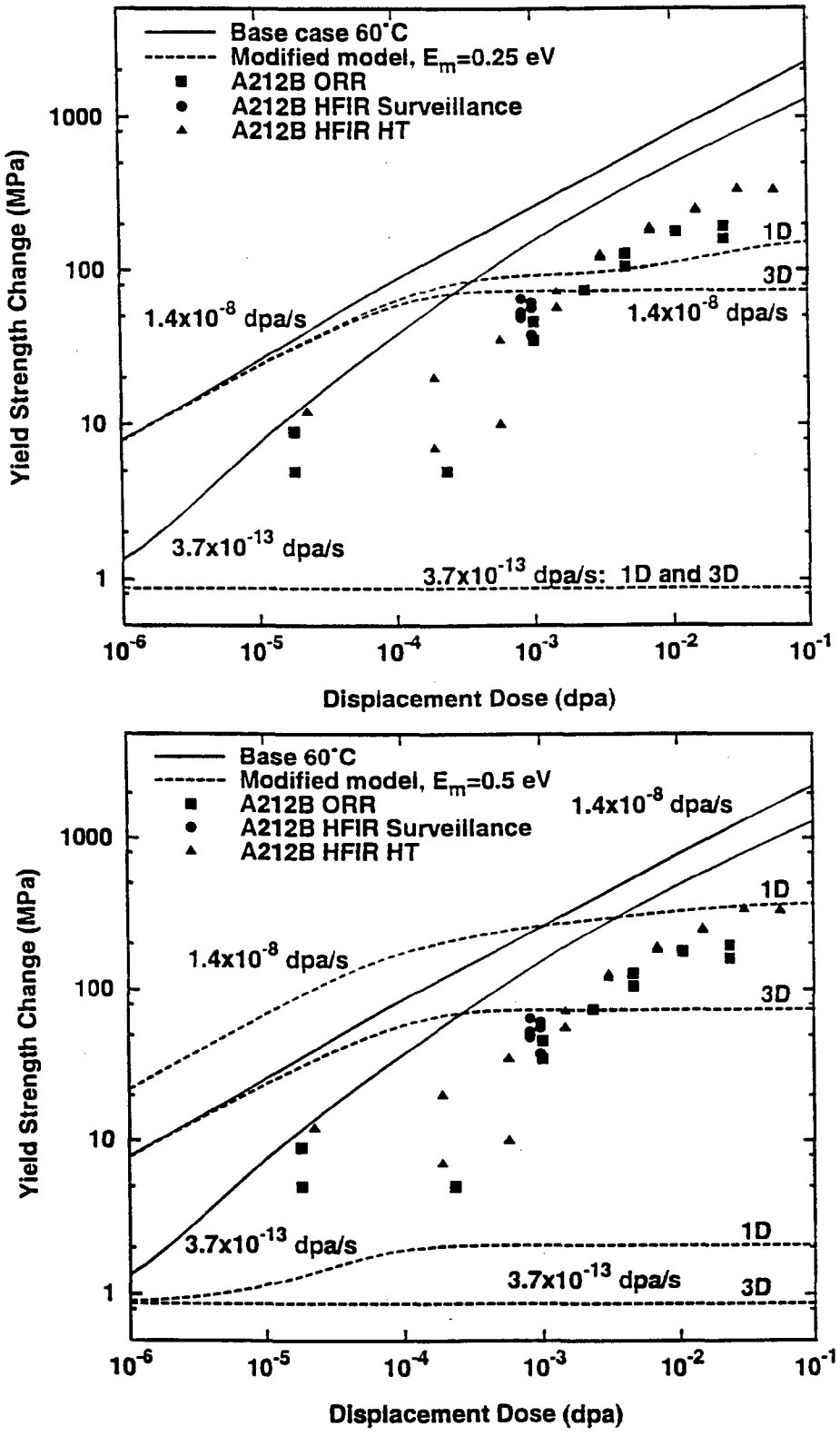

FIG. 5. Comparison of calculated yield strength changes and experimental data for 60°C irradiation at the indicated displacement rates; interstitial cluster migration energy is taken as 0.25 eV in (a) and 0.5 eV in (b).

irradiations was $7x10^{-7}$ dpa/s. The interstitial cluster migration energy is taken as 0.25 eV in part (a) and 0.5 eV in part (b) of Figure 5.

Several observations can be made from the results shown in Figure 5. First, in agreement with the results shown in Figures 3 and 4, the calculated hardening is reduced if the interstitial clusters are mobile. Second, the impact of cluster mobility is somewhat reduced if 1D migration is assumed as opposed to 3D migration. This is more apparent in Figure 5(b) where the higher migration energy leads to greater hardening in either case. This is a result of the reduced effective sink strength for absorbing 1D migrating defects described above. Independent of the assumed mode of migration, the most striking effect is the much greater dependence on the displacement rate observed when the interstitial clusters are mobile. This rate dependence appears because of the lower steady state cluster concentrations that are obtained when the clusters are mobile. Although the previous version of the model tended to predict higher strengthening than indicated by the data, it provides a better fit to the dose dependence of the data.

Results are shown in Figure 6 for an irradiation temperature of 288°C, which is common for commercial reactor RPVs. Values were calculated for two displacement rates; the lower is typical of commercial reactor surveillance programs while the higher is representative of test reactor irradiations; data are shown from irradiations in the University of Virginia Reactor [43]. The effects of cluster mobility are modest at this higher temperature where most of the strengthening is a result of copper-rich precipitates, rather than point defect clusters [7,30]. Cluster mobility leads to less strengthening at doses between ~10^{-3} and 10^{-2} dpa. At the higher displacement rate this leads to somewhat poorer agreement with the dose dependence observed in the test reactor data.

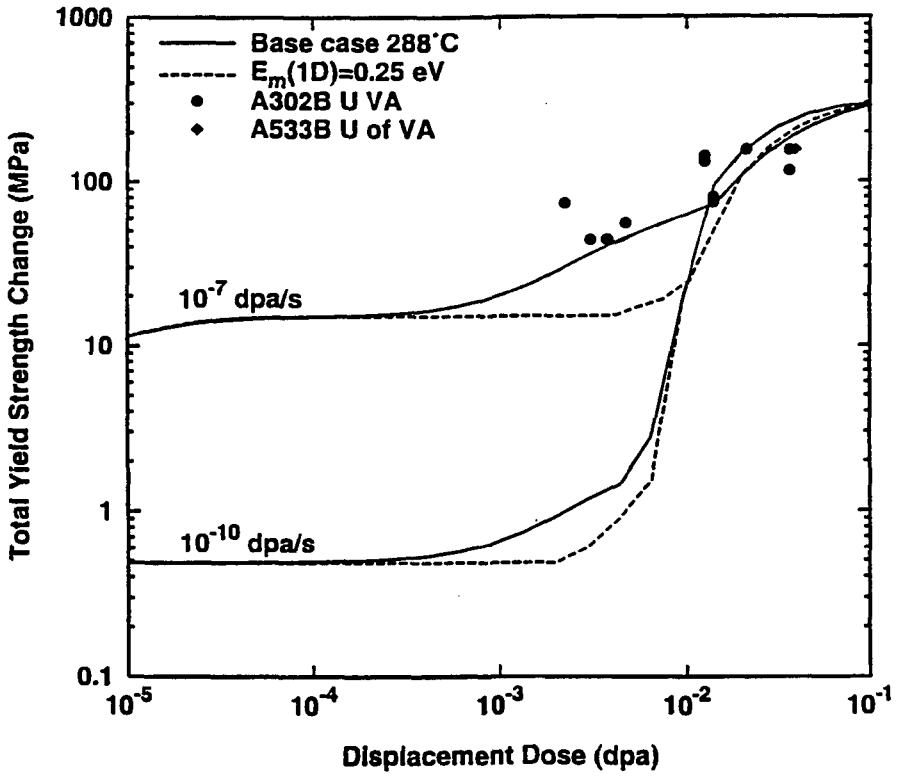

FIG. 6. Comparison of calculated yield strength changes and experimental data for 288°C irradiation at indicated displacement rates; interstitial cluster migration energy is 0.25 eV.

SUMMARY

A previously-developed embrittlement model has been modified to permit an evaluation of the high interstitial cluster mobility that has been observed in molecular dynamics cascade simulations in iron. Simulation of both 1D and 3D cluster migration was investigated. The modifications to include 3D migration were straightforward; sink strengths and cluster-cluster interaction terms were a simple extension of the existing model for 3D migrating point defects. In contrast, because of the approximate nature of the 1D migration model for the required sink strengths, some of the results should be considered preliminary. However, the results obtained with either mode of cluster migration were qualitatively similar.

Cluster migration uniformly led to a reduced cluster sink strength and less radiation-induced hardening for a given set of material parameters. Because of the reduced steady state cluster concentrations, the displacement rate dependence of hardening at doses up to 0.1 dpa was increased, particularly at the lower irradiation temperatures where point defect clusters play a dominant role in hardening. This increased displacement rate dependence at 60°C is not consistent with the data shown in Figure 5 or the data from a larger series of experiments that investigated yield strength changes in ferritic steels over a similar range of displacement rates [42, 44]. The data reported in Refs. 42 and 44 showed essentially no effect of displacement rate in a number of model and engineering alloys irradiated at 60°C at displacement rates between 1.7×10^{-12} and 7×10^{-7} dpa/s. Poorer agreement between the predicted dose dependence of strengthening and the data shown in Figures 5 and 6 was also obtained when the interstitial clusters were mobile. This change was similarly due to the effect of displacement rate on the steady state cluster concentrations.

It is possible that this loss of agreement between model predictions and experimental data could be compensated for by justifiable adjustment of material parameters in the calculations. Specific parameter choices that were required in the initial model to obtain agreement with the data could have acted as a surrogate for interstitial cluster mobility. For example, relatively modest changes in the activation energy for self-diffusion or interstitial migration, or the binding energies of small interstitial clusters can have a large impact on steady state cluster concentrations. However, the increased dose rate dependence arising from cluster mobility is unlikely to be reduced by simple parameter changes. Although a partitioning of the small clusters into sessile and glissile components would reduce the rate dependence, accounting for the mobility of interstitial clusters larger than 4 is likely to increase the rate dependence. Further calculations with more detailed models are needed to investigate these issues.

Alternately, the results could be used to raise a question about the applicability of the MD simulation results. Although the MD results are similar for a range of materials, it must be acknowledged that they only simulate the behavior of a pure material which appears to be mathematically consistent with the target material. Simulations of a pure iron-like material may not adequately represent the actual behavior of engineering ferritic alloys or even of pure iron. The lack of directional bonding in the isotropic, embedded atom type potentials could have significant implications for simulations in transition metals such as iron with strong d-orbital bonding.

The fact that the current embrittlement models do a good job of fitting a broad range of experimental data [7,30,32] could be one argument in favor of neglecting the issue of cluster mobility. However, it seems unlikely that the MD results are substantially in error and this mobility should be accounted for in radiation damage models to the extent possible. This is particularly true of those models which are intended to simulate low-temperature behavior. Additional MD simulations and Monte Carlo simulations can be used to provide more details about the migration behavior of these clusters. For example, in one 20 keV cascade simulation, a gliding 9-interstitial cluster was observed to be trapped by an encounter with a single interstitial after 34 ps, and the cluster was unable to detrap when the simulation was extended for a total of 200 ps [21]. Such cluster trapping could lead to a higher effective migration energy than that observed in short MD cascade simulations and seems even more likely to occur if solutes are present. This would be consistent with the alloy purity effect seen in the work of Eyre and Maher [45] who described the evolution of dislocation loop structures in molybdenum during post-irradiation annealing. Additional MD simulations using alloy potentials should to help answer this question by examining the effects of solute atoms on primary damage formation and defect cluster mobility.

ACKNOWLEDGEMENTS

Research sponsored by the Office of Nuclear Regulatory Research, U.S. Nuclear Regulatory Commission under inter-agency agreement DOE 1886-8109-8L with the U.S. Department of Energy and by the Division of Materials Sciences, U.S. Department of Energy under contract DE-AC05-96OR22464 with Lockheed Martin Energy Research Corporation. The author appreciates helpful reviews by and discussions with S. J. Zinkle and A. F. Rowcliffe.

REFERENCES

[1] A. C. Damask and G. J. Dienes, Point Defects in Metals, Gordon and Breach, 1963.

[2] H. Weidersich, "On the Theory of Void Formation During Irradiation", Radiation Effects 12 (1972) 111-125.

[3] A. D. Brailsford and R. Bullough, "The Theory of Sink Strengths," Philosophical Transactions of the Royal Society of London 302 (1981) 87-137.

[4] L. K. Mansur, "Void Swelling in Metals and Alloys Under Irradiation: An Assessment of the Theory," Nuclear Technology 40 (1978) 5-34.

[5] R. E. Stoller and G. R. Odette, "A Composite Model of Microstructural Evolution in Austenitic Stainless Steel Under Fast Neutron Irradiation," Radiation-Induced Changes in Microstructure, ASTM STP 955, F. A. Garner, N. H. Packan and A. S. Kumar, Eds., American Society of Testing and Materials, Philadelphia, 1987, pp. 371-392.

[6] R. E. Stoller, M. L. Grossbeck, and L. K. Mansur "A Theoretical Model of Accelerated Irradiation Creep at Low Temperatures by Transient Interstitial

Absorption," Effects of Radiation on Materials, ASTM STP 1125, R. E. Stoller, A. S. Kumar, and D. S. Gelles, Eds., American Society of Testing and Materials, Philadelphia, 1992, 517-529.

[7] R. E. Stoller, "Pressure Vessel Embrittlement Predictions Based on a Composite Model of Copper Precipitation and Point Defect Clustering," Effects of Radiation on Materials, ASTM STP 1270, D. S. Gelles, R. K. Nanstad, A. S. Kumar, and E. A. Little, Eds., American Society of Testing and Materials, Philadelphia, 1996, pp. 25-59.

[8] R. E. Stoller, "The Influence of Damage Rate and Irradiation Temperature on Radiation-Induced Embrittlement in Pressure Vessel Steels," Effects of Radiation on Materials, ASTM STP 1175, A. S. Kumar, D. S. Gelles, R. K. Nanstad, and E. A. Little, Eds., American Society of Testing and Materials, Philadelphia, 1993, 394-426.

[9] R. E. Stoller and L. K. Mansur, "The Influence of Displacement Rate on Damage Accumulation During the Point Defect Transient in Irradiated Materials," Radiation Materials Science, Volume 1, Proceedings of International Conference, 1990, Kharkov, Ukraine, pp. 52-67.

[10] R. E. Stoller, "Non-Steady-State Conditions and Incascade Clustering in Radiation Damage Modeling," Journal of Nuclear Materials 244 (1997) 195-204.

[11] P. T. Heald, "The Preferential Trapping of Interstitials at Dislocations, Philosophical Magazine 31 (1975) 551-558.

[12] W. G. Wolfer, "Segregation of Point Defects by Internal Stress Fields," Fundamental Aspects of Radiation Damage in Metals, CONF-751006-P2, U.S. National Technical Information Service, Springfield, VA, 1975, pp. 812-819.

[13] C. H. Woo and B. N. Singh, "The Concept of Production Bias and Its Possible Role in Defect Accumulation under Cascade Damage Conditions," Physica Status Solidi (B) 159 (1990) 609-616.

[14] C. H. Woo and B. N. Singh, "Production Bias due to Clustering of Point Defects in Irradiation-Induced Cascades," Philosophical Magazine A65 (1992) 889-912.

[15] H. Trinkaus, B. N. Singh, and A. J. E. Foreman, "Glide of Interstitial Loops Produced Under Cascade Damage Conditions: Possible Effect on Void Formation," Journal of Nuclear Materials 199 (1992) 1-5.

[16] H. Trinkaus, B. N. Singh, and A. J. E. Foreman, "Impact of Glissile Interstitial Loop Production in Cascades on Defect Accumulation in the Transient," Journal of Nuclear Materials 206 (1993) 200-211.

[17] T. Diaz de la Rubia and W.J. Phythian, "Molecular Dynamics Studies of Defect Production and Clustering in Energetic Displacement Cascades in Copper," Journal of Nuclear Materials 191-194 (1992) 108-115.

[18] A.J.E. Foreman, W.J. Phythian and C.A. English, "The Molecular Dynamics Simulation of Irradiation damage Cascades in Copper Using a Many-Body Potential," Philosophical Magazine A66 (1992) 671-695.

[19] A.F. Calder and D.J. Bacon, "A Molecular Dynamics Study of Displacement Cascades in Iron," Journal of Nuclear Materials 207 (1993) 25-45.

[20] W. J. Phythian, R. E. Stoller, A. J. E. Foreman, A. F. Calder, and D. J. Bacon, "A Comparison of Displacement Cascades in Copper and Iron by Molecular Dynamics and its Application to Microstructural Evolution," Journal of Nuclear Materials 223 (1995) 245-261.

[21] R. E. Stoller, "Molecular Dynamics Simulations of High Energy Cascades in Iron," Microstructure of Irradiated Materials, I. M. Robertson, L. E. Rehn, S. J. Zinkle, and W. J. Phythian, Eds., Materials Research Society, Pittsburgh, PA, 1995, pp. 21-26.

[22] R. E. Stoller, "Point Defect Survival and Clustering Fractions Obtained from Molecular Dynamics Simulations of High Energy Cascades," Journal of Nuclear Materials 233-237 (1996) 999-1003.

[23] D.J. Bacon and T. Diaz de la Rubia, "Molecular Dynamics Computer Simulations of Displacement Cascades in Metals," Journal of Nuclear Materials 216 (1994) 275-290.

[24] D.J. Bacon, A. F. Calder, F. Gao, V. G. Kapinos, and S. J. Wooding, "Computer Simulation of Defect Production by Displacement Cascades in Metals," Nuclear Instruments and Methods in Physics Research B102 (1995) 37-46.

[25] M. J. Norgett, M. T. Robinson, and I. M. Torrens, "A Proposed Method of Calculating Displacement Dose Rates," Nuclear Engineering and Design 33 (1975) 50-54.

[26] B. D. Wirth, G. R. Odette, D. Maroudas, and G. E. Lucas, "Energetics of Formation and Migration of Self-Interstitials and Self-Interstitial Clusters in alpha-iron," Journal of Nuclear Materials 244 (1997) 185-194.

[27] R. E. Stoller, G. R. Odette, and B. D. Wirth, Journal of Nuclear Materials 251 (1997) 49-60.

[28] B. D. Wirth, G. R. Odette, D. Maroudas, and G. E. Lucas, "Simulation of Interstitial Cluster Mobility and Cluster Mediated Surface Topologies," presented in Symposium KK at the December 1997 meeting of the Materials Research Society, Boston, MA, to be published.

[29] U. Gösele and A. Seeger, "Theory of Bimolecular Reaction Rates Limited by Anisotropic Diffusion," Philosophical Magazine 34 (1976) 177-193.

[30] G. R. Odette, "On the Dominant Mechanism of Irradiation Embrittlement of Reactor Pressure Vessel Steels," Scripta Metallurgica 17 (1983) 1183-1188.

[31] G. R. Odette and C. K. Sheeks, "A Model for Displacement Cascade Induced Microvoid and Precipitate Formation in Dilute Iron-Copper Alloys," Phase Stability During Irradiation, J. R. Holland, L. K. Mansur, and D. I. Potter, Eds., The Metallurgical Society of the AIME, Warrendale, PA, 1981, pp. 415-436.

[32] S. B. Fisher, J. E. Harbottle, and N. Aldridge, "Radiation Hardening in Magnox Pressure-Vessel Steels," Philosophical Transactions of the Royal Society of London A315 (1985) 301-322.

[33] K. C. Russell and L. M. Brown, "Dispersion Strengthening in Iron-Copper System," Acta Metallurgica 20 (1972) 969-974.

[34] G. E. Lucas, G. R. Odette, P. M. Lombrozo, and J. W. Sheckherd, "Effects of Composition, Microstructure, and Temperature on Irradiated Hardening of Pressure Vessel Steels," Effects of Radiation on Materials, ASTM STP 870, F. A. Garner and

J. S. Perrin, Eds., American Society of Testing and Materials, Philadelphia, 1985, pp. 900-930.

[35] F. W. Stallman, Jy-An Wang, F. B. K. Kam, and B. J. Taylor, PR-EDB: Power Reactor Embrittlement Data Base, NUREG/CR-4816 Revision 2, ORNL/TM-10328/R2, Oak Ridge National Laboratory, Oak Ridge, TN, 1994.

[36] R. E. Stoller, "The Role of Point Defect Clusters in Reactor Pressure Vessel Embrittlement," Environmental Degradation of Materials In Nuclear Power Systems: Water Reactors, Sixth International Symposium, R. E. Gold and E. P. Simonen, Eds., The Metallurgical Society, Warrendale, PA, 1993, pp. 747-754.

[37] W. M. Lomer and A. H. Cottrell, "Annealing of Point Defects in Metals and Alloys," Philosophical Magazine 46 (1955) 711-719.

[38] C. H. Woo and W. Frank, "A Theory of Void Lattice Formation," Journal of Nuclear Materials 137 (1985) 7-21.

[39] B. N. Singh, S. I. Golubov, H. Trinkaus, A. Serra, Yu. N. Osetsky, and A. V. Barashev, "Aspects of Microstructure Evolution Under Cascade Damage Conditions," Journal of Nuclear Materials 251 (1997) 107-122.

[40] H. Weidersich, "Evolution of Defect Cluster Distributions During Irradiation," Physics of Irradiation Effects in Metals PM'91, G. Szenes, Ed., Materials Science Forum 97-99, Trans. Tech. Publications, Zürich, 1992, pp. 59-73.

[41] R. D. Cheverton, J. G. Merkle, and R. K. Nanstad, "Evaluation of HFIR Pressure Vessel Integrity Considering Radiation Embrittlement," ORNL/TM-10444, Oak Ridge National Laboratory, April 1988.

[42] R. E. Stoller, K. Farrell, and L. K. Mansur, "The Effect of Thermal Neutrons and Fast Flux on Tensile Properties of Ferritic Steels Irradiated at Low Temperature," ORNL/NRC/LTR-96/3, Oak Ridge National Laboratory, 1996.

[43] G. R. Odette and G. E. Lucas, "Irradiation Embrittlement of LWR Pressure Vessel Steels," EPRI NP-6114, Electric Power Research Institute, Palo Alto, CA 1989.

[44] G. R. Odette, G. E. Lucas, R. D. Klingensmith, R. E. Stoller, and W. J. Phythian, "On the Effect of Flux and Composition on Irradiation Hardening at 60°C," Effects of Radiation on Materials, ASTM STP 1270, D. S. Gelles, R. K. Nanstad, A. S. Kumar, and E. A. Little, Eds., American Society of Testing and Materials, Philadelphia, 1996, pp. 547-568.

[45] B. L. Eyre and D. M. Maher, "Neutron Irradiation Damage in Molybdenum: Part V," Philosophical Magazine 24 (1971) 767-797.

Report Number (14) ORNL/CP--98106
CONF-960643--

Publ. Date (11) 199805
Sponsor Code (18) DOE/ER, XF
UC Category (19) UC-400, DOE/ER